

MAGNETIC DESIGN OF THE LNLS TRANSPORT LINE

R. H. A. Farias, Liu Lin and G. Tosin, LNLS, Campinas, SP 13081-970 BRAZIL

The transport line for the injection system of the LNLS UVX storage ring is described. The line connects an underground 100 MeV LINAC to the 1.15 GeV UVX electron storage ring. The designs for the magnets are reviewed and the measurements of the prototypes are presented.

I. INTRODUCTION

The magnetic lattice of the transport line consists of a quadrupole doublet just after the underground LINAC, an achromatic vertical translation which brings the beam to the ring level and a horizontal achromatic deflection, including the septa, which leads the beam to the injection point [1]. Although the injection energy is chosen to be 100 MeV, the line has been designed for 250 MeV electron energy, allowing for future upgrade of the injection system either by recirculating the beam in the LINAC or by using SLED.

The transport line is 20.031 m long, including the septa. A lay-out is shown in figure 1. The line presents some flexibility for optical function matching. Presently it can be operated either with the optical functions matched to the storage ring functions, or with the functions mismatched so that the injected beam ellipse occupies the maximum area in the available storage ring acceptance. The vacuum chamber will be cylindrical, with inner diameter $\varnothing=35$ mm. This limits the maximum beam energy deviation in the line to $\pm 1.6\%$ since the maximum dispersion function is 1.09 m. The dipole chambers will be squeezed to 24 mm (inner dimension) in the gap direction, which does not decrease the beam stay-clear.

The line is made up of 4 dipoles, 12 quadrupoles and 2 septa. Additional coils in the quadrupoles and trim coils in the dipoles will be used as built-in steering elements. This

choice makes alignment and supports easier. The dipoles can be used to correct the orbit in their respective bending planes, whereas the quadrupoles can be used to correct in both planes.

Simulations of orbit distortion and correction for the matched injection mode have shown that the beam path can be kept within ± 1.5 mm displacement for maximum steering strengths of ± 3 mrad (including a 50% safety margin). The steering coils are designed to provide this steering strength at the energy injection of 250 MeV.

All the transport line magnets have been designed with the 2D POISSON [2] package. The precision in the lamination dimensions as determined by the laser cutting process has been simulated in the design project of the magnets. Both the precision and the roughness of the cut are of the order of $\pm 25\mu\text{m}$.

II. SEPTA

The final deflection of the injected beam towards the storage ring will be carried out by two septa deflecting the beam in the plane of the stored beam orbit. The parameters for these magnets are shown in table 1 [3,4].

Both septa are conventional non-staggered laminated C-core d.c. magnets (figures 2-3). The yokes are composed of stacks of 1.5 mm thick low coercivity (1.0 Oe) low carbon steel laminations kept together by tie rods, without special end plates. The thick septum consists of two pieces aligned to each other by means of a precision dowel pin in a V groove and held together by means of aluminum clamps (figure 3). The magnetic field in these magnets is

Table 1 - Parameters for the transport line septa (@250 MeV).

	Thin septum	Thick septum
Deflection	3°	15°
ρ (m)	15.33	3.83
Magnetic length (m)	0.8027	1.0027
Physical length (m)	0.7744	0.9413
Gap (mm)	21	44
B (T)	0.054	0.218
Good field width (mm)	41	166
Septum thickness (mm)	5.0	50
Number of turns	4	264
Current (A)	227	30
Voltage (V)	3.3	21
Power (W)	750	630
Inductance (mH)	0.05	600

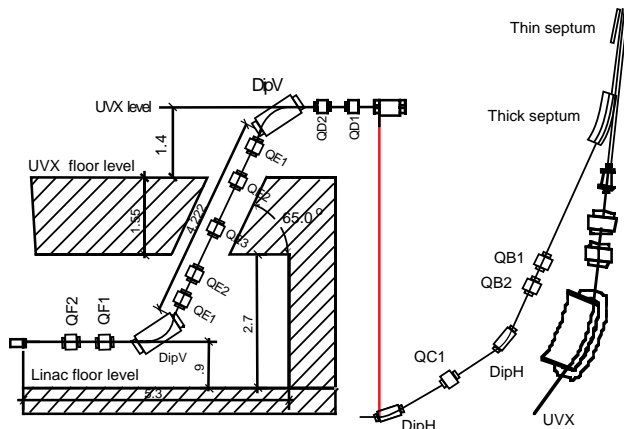


Figure 1 - LINAC-UVX transport line: magnetic lattice.

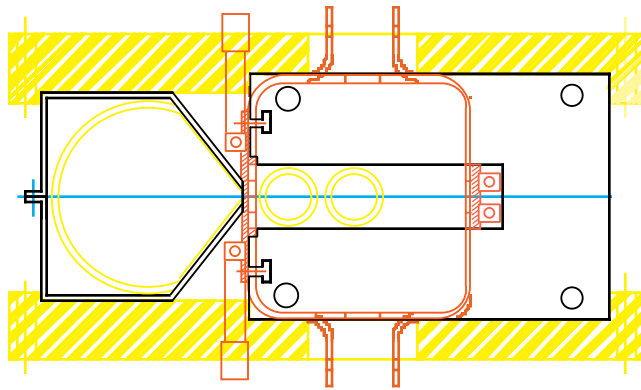


Figure 2 - Transverse cut of the thin septum. The core and the magnetic shield are inlaid in an aluminum box used for support and alignment.

low —even for the highest energy injection— and no ‘chamfering’ has been introduced in the longitudinal pole profile.

The coils are made of solid copper conductors with rectangular cross sections. For the thin septum coil an efficient cooling system is of paramount importance. For the injection energy of 250 MeV, the power dissipated in the septum wall is of the order of 270 W and the current density reaches 23 A/mm². The four turns of the coil are assembled on a water cooled brass support.

For the thick septum, the coil is a unique package of 264 turns of non-water cooled copper conductor encapsulated in insulation varnish. The maximum current

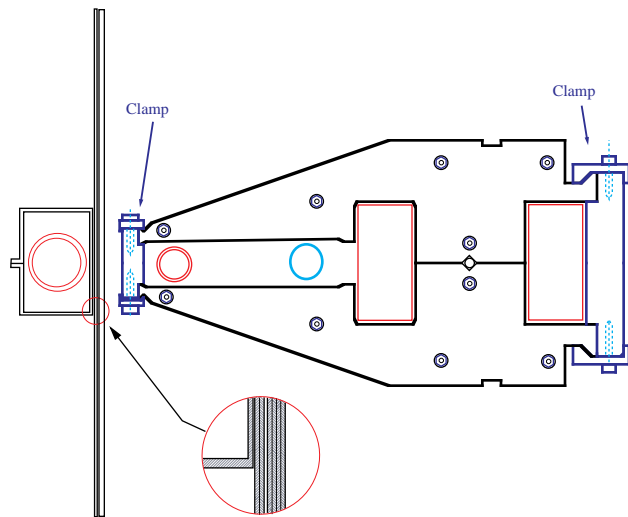


Figure 3 - Thick septum: transverse cut.

density in the most demanding conditions is 1.7 A/mm².

The thin septum has been assembled and measured. Measurements obtained using a Hall probe have shown good agreement with the numerical simulations (Figure 4). The screening of the magnetic field in the storage ring vacuum chamber region satisfies the design specifications. Measurements of the lateral fringing field have shown a

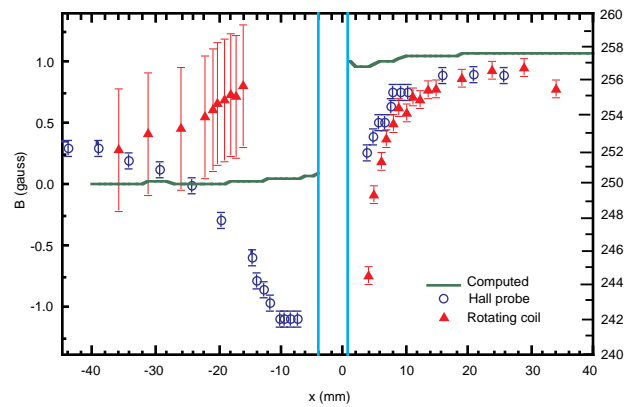


Figure 4 - Thin septum: measured and computed fields. At left, the field inside the stored beam region. At right the field inside the septum gap. The scales are different for the two regions. The measurements correspond to the injection energy of 120 MeV ($I=108.9$ A).

maximum remanent field of 1.1 gauss for 120 MeV injection energy. Measurements of the integrated longitudinal field using the rotating-coil technique show a difference of approximately 0.3% as compared to the hard-edge model. In this case the coil has shown excellent thermal behaviour. For 250 MeV injection energy, modifications will be required in the cooling system of the coil.

III. DIPOLES

The four bending magnets of the transport line are grouped into two families (Table 2)[5]. These dipoles are standard C-core magnets consisting of 1.5 mm thick laminations stacked and held together by tie rods. Special

Table 2 - Parameters for the transport line dipoles (@250 MeV).

	Vertical	Horizontal
# of elements	2	2
Deflection	65°	33°
ρ (m)	0.80	0.80
Magnetic length (m)	0.9076	0.4608
Physical length (m)	0.8997	0.4544
Gap (mm)	30.0	30.0
B (T)	1.04	1.04
Good field width (mm)	20.0	125.3
Number of turns	460	460
Current (A)	28.1	28.4
Voltage drop (V)	64.1	44.8
Power (kW)	1.8	1.27
Inductance (H)	3.9	2.6

20 mm thick laminations of non-ferromagnetic stainless steel are used as end plates.

The laminations for the vertical deflection dipoles are staggered due to the large deflection angle and to the geometrical constraints in the transport line. In order to prevent non-linear effects due to saturation of the magnetic field in the core corners, the ends of both dipoles have been rolled off. The longitudinal profile of the poles have a 30 mm radius circular chamfer.

The coils for the dipoles are constructed as flat pancakes with two layers of solid copper conductors amounting to 92 windings each pancake. Each pancake is wrapped with insulation polyester tape and impregnated with insulation varnish. Each dipole holds two coils, which in turn is composed of five pancakes. The built-in steering capabilities are attained by supplying additional trim coils wound along the backleg of the dipoles. Using 16 mm² cross section extra-flexible copper wire, the magnetic field required for the maximum deflection of 3.0 mrad can be reached with 8 windings for the vertical and 16 windings for the horizontal dipoles (for a current of ± 9.8 A).

According to numerical simulations, the transversal field homogeneity along the good field region is $4 \times 10^{-3}\%$ for the vertical dipole and $5 \times 10^{-2}\%$ for the horizontal one.

IV. QUADRUPOLES

There are 12 quadrupoles in the transport line [6]. They are composed of four identical parts, each one corresponding to a pole. This is particularly suitable for the shuffling of the laminations which provides better uniformity of the magnetic characteristics. The laminations are stacked without end plates and held together by tie rods.

Table 3 - Parameters for the transport line quadrupoles (@250 MeV).

# of elements	12
Maximum Gradient (T/m)	5.1
Magnetic aperture radius (mm)	20.0
Magnetic length (m)	0.2
Gap (mm)	30.0
B (T)	1.04
Good field width (mm)	20.0
Number of turns/coil (main coil)	72
Maximum Current (A)	12
Maximum Voltage drop (V)/mag.	3.7
Power (W)	44
Inductance (mH)	43

Each main coil is composed by 80 mechanical windings. Neither the main or the steering coils are water cooled.

The tolerance for the maximum relative deviation of the magnetic field profile from a pure quadrupole field is 5.0×10^{-3} at the internal wall of the vacuum chamber. Simulations show for the transport line quadrupoles an expected maximum relative deviation of the order of 5.0×10^{-4} .

V. CONCLUSIONS

We have presented the design project for the transport line from the LNLS LINAC to the UVX storage ring, including a brief description of the lattice and the magnetic design of all components. Among these, in our case, the thin septum was the most critical item. The results of its magnetic, mechanical and thermal characterization showed, however, that the constructed piece characteristics is within the required tolerances. Simulations have shown that besides the mechanical tolerances of the laminations, the septum coil positioning precision is as well a critical parameter for the field quality. This is probably the main reason for the small differences between the measured and the simulated fields near the septum wall.

The thick septum laminations are already cut as well as part of the quadrupoles. They will be assembled in the near future. The remaining transport line magnets will be constructed and characterized by August 1995.

VI. REFERENCES

- [1] Liu Lin, "Updated LINAC to UVX transport line", LNLS CT-01/95, 1995.
- [2] Reference Manual for the POISSON/SUPERFISH Group of Codes, Los Alamos Accelerator Code Group, LA-UR-87-126.
- [3] A. R. D. Rodrigues and R. H. A. Farias, "Projeto Magneto-mecânico de um Septum Fino D.C.", LNLS CT-15/94, 1994.
- [4] A. R. D. Rodrigues and R. H. A. Farias, "Projeto do Septum Grosso D.C.", LNLS CT-02/95, 1995.
- [5] A. R. D. Rodrigues and R. H. A. Farias, "Projeto dos Dipolos da Linha de Transporte", LNLS CT-12/95, 1995.
- [6] A. R. D. Rodrigues and R. H. A. Farias, "Projeto dos Quadrupolos da Linha de Transporte", LNLS CT-13/95, 1995.